

Estimating the acceleration of transformer aging due to electric vehicle charging

Alexander D. Hilshey, *Student Member, IEEE*, Paul D. H. Hines, *Member, IEEE*, Jonathan R. Dowds

Abstract—This paper describes a method for estimating the additional aging in medium/low voltage distribution transformers caused by increasing demand from electric vehicle charging. The proposed method combines detailed travel demand data from the National Household Transportation Survey with a one-year model of transformer hottest spot temperature, based on IEEE C57.91-1995 Annex G. To illustrate the model outputs, we present results for 15kVA and 25kVA overhead distribution transformers using ambient temperatures from Burlington, VT and Los Angeles, CA. Our results illustrate the importance of ambient temperatures to impact of PEVs on transformer aging.

Index Terms—Plug-in hybrid electric vehicles, transformer aging

NOMENCLATURE

B	Constant in viscosity calculation
C	Constant in viscosity calculation
dt	Time step in minutes
EQA	Equivalent aging in hours
E_{WHS}	Eddy loss at hottest spot, per-unit
F_{AA}	Factor of accelerated aging
F_{EQA}	Factor of equivalent aging
H_{HS}	Height of hottest spot location, per-unit
K_{HS}	Temperature correction for losses at hottest spot location
K_W	Temperature correction for losses of windings
L	Per-unit load
M_{CORE}	Mass of core
M_{OIL}	Mass of oil
M_{TANK}	Mass of tank
$M_W C_{PW}$	Winding mass times specific heat of winding material in watt-min/C.
P_C	Core loss in watts
P_E	Winding eddy loss in watts
P_{EHS}	Eddy loss at rated hottest spot temperature in watts
P_S	Stray losses in watts
P_{WHS}	Winding I^2R at rated hottest spot temperature in watts
P_W	Winding I^2R loss in watts
Q_C	Heat generated by core in watt-min
$Q_{GEN,HS}$	Heat generated at hottest spot in watt-min
$Q_{GEN,W}$	Heat generated by windings in watt-min

$Q_{LOST,HS}$	Heat lost at hottest spot in watt-min
$Q_{LOST,OIL}$	Heat lost by the oil in watt-min
$Q_{LOST,W}$	Heat lost by the winding in watt-min
Q_S	Heat generated by stray losses in watt-min
T_A	Ambient temperature in degrees Celsius
$T_{A,R}$	Rated ambient temperature in degrees Celsius
T_{BO}	Bottom oil temperature in degrees Celsius
$T_{BO,R}$	Rated bottom oil temperature in degrees Celsius
T_{DAO}	Average oil temperature in cooling ducts in degrees Celsius
$T_{DAO,R}$	Rated average oil temperature in cooling ducts in degrees Celsius
T_{HS}	Hottest spot temperature in degrees Celsius
$T_{HS,R}$	Rated hottest spot temperature in degrees Celsius
T_K	Temperature factor for resistance correction in degrees Celsius
T_O	Average oil temperature in degrees Celsius
$T_{O,R}$	Rated average oil temperature in degrees Celsius
T_{TDO}	Oil temperature at top of cooling ducts in degrees Celsius
$T_{TDO,R}$	Rated oil temperature at top of cooling ducts in degrees Celsius
$T_{TO,R}$	Rated top oil temperature in degrees Celsius
T_W	Average winding temperature in degrees Celsius
$T_{W,R}$	Rated average winding temperature in degrees Celsius
$T_{WO,R}$	Rated oil temperature adjacent to hottest spot location in degrees Celsius
Z	Exponent for duct oil rise over bottom oil
ΔT_{TB}	Oil temperature rise at top of cooling duct to bottom in degrees Celsius
ΔT_{WO}	Oil temperature rise at hottest spot location to bottom in degrees Celsius
μ_{HS}	Viscosity of fluid for hottest spot calculation
$\mu_{HS,R}$	Viscosity of fluid for rated hottest calculation at rated load
μ_W	Viscosity of fluid for average winding temperature rise calculation
$\mu_{W,R}$	Viscosity of fluid for average winding temperature rise calculation at rated load
τ_W	Winding time constant in minutes

I. INTRODUCTION

WITH several mass-market plug-in hybrid and battery electric vehicles, collectively plug-in electric vehicles (PEVs), currently for sale or scheduled to go on sale in the 2012 and 2013 model years, there is a growing need to assess the impact that PEV charging load will have on electricity

This work is supported in part by the Transportation Research Center at the University of Vermont, through a grant from the U.S. Dept. of transportation.

A. Hilshey and P. Hines are with the School of Engineering, University of Vermont, Burlington, VT (e-mail: ahilshey@uvm.edu; paul.hines@uvm.edu).

J. Dowds is with the Transportation Research Center, University of Vermont, Burlington, VT (e-mail: jdowds@uvm.edu).

distribution infrastructure. Substantial research already exists regarding the regional and national impact of PEVs on gasoline consumption [1], [2], [3], [4], power-plant emissions [1], [2], [5], [6], electricity costs [7], [8], [9], and generating supply adequacy [10], [11], [9]. These studies universally found that increasing PEV deployment reduced petroleum consumption. The majority of the studies listed above also concluded that PEV use reduced net greenhouse gas emissions and several studies found a no change or a net decrease in overall NOx emissions. Price impacts and supply adequacy findings are highly sensitive to assumptions about the timing of PEV charging, but there is a strong consensus in the literature that, at least from a technical perspective, the impacts on peak electric demand (and therefore required generation capacity) could be effectively managed through controlled or “smart charging” [10], [2], [4], [9]. To date, the literature on medium and low distribution system impacts, discussed in Section 1.1, is relatively limited and offers very little guidance to utilities looking to incorporate PEV impacts into their maintenance and investment strategies for these systems.

Several factors combine to make quantifying the impact of PEVs on the medium and low voltage distribution infrastructure a particularly pressing issue. First, the social benefits offered by PEV deployment in terms of reduced oil consumption and life-cycle greenhouse gas emissions have prompted numerous policies at both the state and federal levels that are geared towards increasing the rate of PEV adoption [12], [13], [14], [15]. Second, because early PEV adopters are likely motivated at least in part by environmental concerns, and because there is evidence from past hybrid electric vehicle sales that environmentally motivated vehicle consumers tend to be geographically clustered [16], it is likely the PEV sales will be concentrated in particular areas. This clustering effect makes it highly probable that PEVs will impact local distribution infrastructure well before the additional charging load impacts transmission or generation infrastructure. If, as is suggested in [17], these impacts are severe, distribution utilities may have to make significant infrastructure investments to adapt to this new load. Accurate information on PEV impacts will be essential for ensuring that these investments are made in an efficient manner.

Thus the goal of this paper is to present, and illustrate the utility of, a computational method for estimating the additional transformer aging of increasing PEV load.

A. Background on transformer modeling and the distribution system impacts of PEVs

Though the research suggests that off-peak periods could be used to support a national fleet of PHEVs with little need to increase national grid delivery capacity[18], there is conflicting evidence regarding the impact of PEVs on the residential distribution infrastructure. Roe et al. [17] use a time-series model of transformer aging and argue that PEV charging could decrease transformer life by 93%. The study results, however, are based on a model from [19] which does not reflect the state of the art in transformer modeling. Another study suggests that a penetration level as small as 10% could overload

overhead distribution transformers[20]. Fernández et al. [21] analyze two residential distribution circuits and estimate that distribution infrastructure costs could increase by 19% and energy losses could increase by 40% with substantial PEV deployment. It should be noted that these costs could be offset by increased revenues from PEV-related demand, and that the scale of the infrastructure impacts depend on the charging method employed. On the other hand, the results of [18] suggest that the impacts of PHEV charging on components of residential feeders could be minimal if smart charging is employed, and Clement-Nyns et al. [22] argue that PEV deployment with smart charging could have net benefits for the distribution system by leveling power demand and thus reducing distribution losses per unit energy.

Transformers are among the most costly components in the medium/low voltage distribution infrastructure and, therefore, transformer aging is a key consideration when evaluating the impacts of PEV charging. Transformer life is highly dependent on the state of internal insulation degradation, which is dependent on internal transformer temperatures. Accurately modeling transformer temperatures is crucial to accurately predict transformer aging. IEEE Standard C57.91 [23] describes methods to estimate a transformer’s hottest spot temperature given ambient temperatures and loading profiles.

There is some debate in the literature about the accuracy of the some of the details in IEEE C57.91 [24], [25], [26]. Test data from [25] suggest that the simplest version of the top oil rise over ambient temperature model is not accurate for longer time-series analysis. These inaccuracies stem from the fact that the body of the standard assumes that ambient temperature is a static value. The authors of [26] concur with this conclusion. Pierce [24] also argues for more detailed treatment of time-varying ambient temperatures, and provides a detailed thermodynamic model of transformer temperatures and fluid flows during transient conditions. The model in [26] is substantially simpler than that in [24]. To our knowledge there is no existing empirical work comparing the relative accuracies of the models in [24] and [26]. The 1995 revision of IEEE C57.91 [23] includes an appendix (Annex G) that details the method in [24]. The improved transformer loading equations consider the cooling fluid type, resistance and fluid viscosity changes with temperature, as well as ambient temperature and load variation. The model described in Annex G is not, to our knowledge, contested in the existing literature. Therefore the work described in this paper is based on IEEE C57.91 Annex G.

B. Background on the modeling of PEV power demand

Accurately estimating the impact of PEV charging on components of the distribution infrastructure from time-series data requires both good physical models of circuit components (see above) and good estimates of the electric power demand due to PEV charging. Early PEV research assumed very simple charging profiles [2], [27], [4], [9], such as assuming that vehicles will charge daily at 5, 6 or 7 pm, with batteries fully depleted at the beginning of each charge cycle. Gonder et al. [3] propose a model of electric demand from 20 and 40 mile

range PHEVs using GPS data from a small fleet of light-duty vehicles which has been used by several subsequent authors. Wu et al. [28] proposed a probabilistic model that produces charging profiles based on US travel survey data. Our method uses the same National Household Travel Survey data [29] as [28], with a slightly different sampling strategy.

C. Outline of the contributions in this paper

Building on this existing research, the goal of this paper is to model the transformer aging impact of PEV charging, given an accurate time-series transformer model, hourly ambient temperature data and PEV demand profiles derived from observed light-duty vehicle travel patterns. Section 2 describes the modeling method in detail. Our results (Sec. 3) illustrate the important effects of thermal climate (ambient temperature) and PEV demand on expected transformer life. Sec. 4 summarizes our conclusions and goals for future work.

II. PEV TRANSFORMER IMPACT MODEL

The purpose of the PEV transformer impact model (PTIM) is to estimate the aging effects that PHEV charging imposes on overhead distribution transformers. In this paper we use PTIM to evaluate transformer aging over a period of one year and use ambient temperature data from two distinct climates, Vermont and Southern California. Fig. 1 shows the inputs and outputs of PTIM in block diagram form. In summary the model requires as inputs: an hourly baseline demand profile for the transformer derived from the number of homes connected to the transformer, a PEV charging demand profile, hourly ambient temperatures, and detailed transformer specifications. The output of the model is the lose of transformer life that results from transformer hottest spot temperatures, in years. Normally, for a moderately loaded residential service transformer, loss-of-life (equivalent aging) is substantially less than one year over a one year period. The transformer demand profile is produced by adding the PEV charging load and the baseline load. The transformer temperature model, which is based on the model from Annex G of [23], uses the PEV demand profile and the temperature data as inputs to evaluate the transformer hottest spot temperature. Finally, the transformer hottest spot temperature is translated to equivalent aging of the transformer in years, or a factor of equivalent aging to be used for comparison against rated transformer aging.

A. Baseline Demand Profiles

The baseline demand profile was developed based on single residence hourly load curves from [30] as interpreted by [20]. The load value of each hour of the daily load curve was entered into a vector in MATLAB. Load was assumed to be constant throughout the year so each of the 24 load values in this vector was repeated for 365 days. The result is an 8760×1 vector containing load values for each hour in a calendar year. Finally, MATLAB interpolated over 60 data points per hour, resulting in a new vector with interpolated load data for every minute of the year. All homes were assumed to have identical load curves

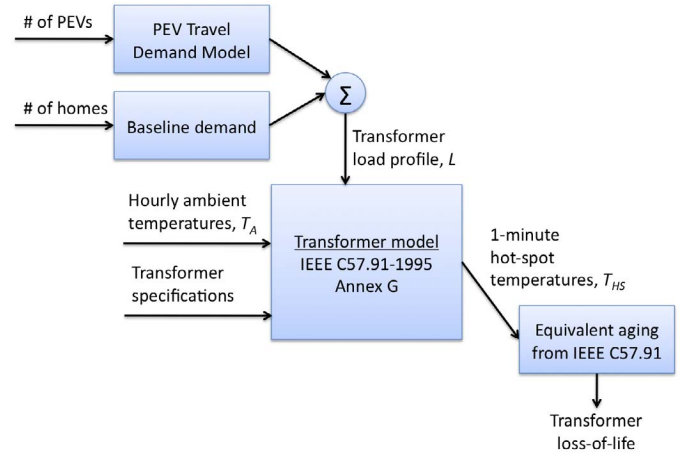


Figure 1. Illustration of the inputs and outputs of the PEV Transformer Impact Model

so baseline demand profiles for various numbers of houses were created by multiplying the single household vector by the desired number of houses. Fig. 2 shows the demand profiles used in this paper.

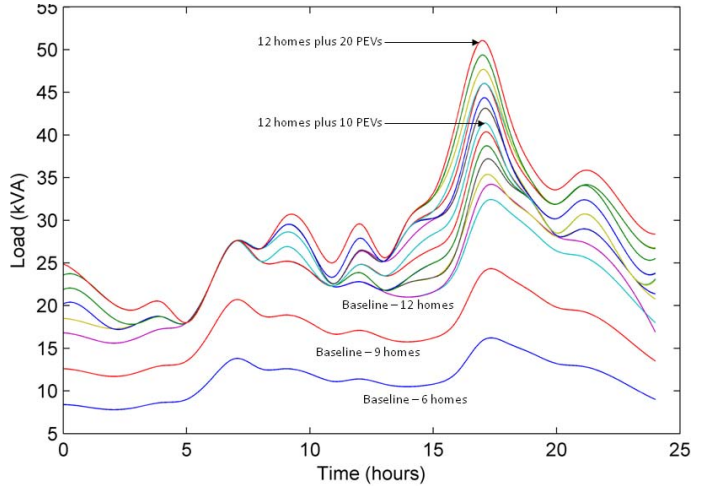


Figure 2. Daily demand profile. Baseline demand profiles are shown for 6, 9, and 12 homes. Additional load from PEVs are added to each of the baseline demand profiles. This is demonstrated in this figure by adding additional PEV load to the baseline demand profile for 12 homes.

B. Additional Demand from PHEV Charging

The additional hourly load required for vehicle charging was derived from the National Household Travel Survey (NHTS), a comprehensive survey of US travel patterns conducted by the Federal Highway Administration [29]. The survey data includes all trips taken by all members of the household within a 24 hour period including the length, timing, duration and mode of transportation for each trip. From this data set, we randomly selected weekday travel records for twenty cars where the car both began and ended the survey period at home. Each vehicle record was randomly assigned to one of the three plug-in hybrid electric vehicle (PHEV) profiles shown in Table 1. These profiles were created based on

performance characteristics for the Chevrolet Volt [31], the Fisker Karma [32], and the BYD F3DM [33], which began selling in China in 2008 reported by the vehicle manufacturers and the popular press. The Volt, Karma and F3DM are all series hybrid vehicles so operate in straight charge depleting mode (i.e., entirely under battery electric power) until the limit of their all-electric range (AER) and then to switch to charge sustaining mode and derive all of their energy from gasoline.

Table I
VEHICLE CHARACTERISTICS

	Electric Drive Efficiency (kWh/miles)	All-electric Range (miles)
Volt	.220	40
Karma	.323	50
F3DM	.256	68

To calculate the additional charging load, all PHEVs were assumed to be able to charge at home and to charge there exclusively. Charging was assumed to begin immediately upon the vehicle's return home and to continue until the battery reach its capacity or the vehicle began a new trip. Vehicles could charge for fractions of an hour before and after trips but a vehicle was assumed not to charge between trips if it started a subsequent trip in the same hour that it ended prior trip. Once a vehicle returned home for the final time in the 24 hour survey period, it was assumed to be available to charge until 5 AM the next morning. Vehicle charge rate was assumed to take place at 1.44 kW [34] and to be 85% efficient. We ran this selection and load calculation process ten times and selected the load profile which was closest to the average values from the ten runs for peak demand and total load.

C. Transformer Temperature Model

The transformer temperature model estimates the internal transformer temperatures using the *Alternative Temperature Calculation* method proposed in Annex G of IEEE C57.91-1995. The transformer temperature model uses forward Euler integration to estimate the internal transformer temperatures at one minute intervals.

Transformer aging results from transformer insulation break-down, which is directly related to the temperature of the transformer windings. Therefore, the winding hottest spot temperatures, estimated by this model, are needed to determine the equivalent aging of the transformer. The transformer temperature model uses the procedure from [23], outline below, to estimate the winding hottest spot temperatures at each time interval.

1) *Average Winding Temperature Calculations:* In addition to load and ambient temperature, initial conditions for average winding temperature, T_W ; bottom oil temperature, T_{BO} ; and oil temperature at top of duct, T_{TDO} , are required to estimate the the parameters described below. With these parameters, it is possible to estimate the average winding temperature at the current time step.

The first calculated parameter, $T_{DAO,1}$, is the oil temperature at the top of the cooling duct at the current time step:

$$T_{DAO,1} = \frac{(T_{BO,1} + T_{TDO,1})}{2} \quad (1)$$

where T_{BO} and T_{DO} are the initial conditions for the first time step or the values calculated in the previous step for subsequent time steps.

Eq. 2 estimates the viscosity of the oil for average winding temperature rise above ambient temperature, μ_W , at the current time step:

$$\mu_{W,1} = B e^{C / \left(\left(\frac{T_{W,1} + T_{DAO,1}}{2} \right) + 273 \right)} \quad (2)$$

where B and C are constants for the viscosity equation given in . Eq. 3 estimates the rated viscosity of the oil for average winding temperature rise above ambient temperature, $\mu_{W,R}$:

$$\mu_{W,R} = B e^{C / \left(\left(\frac{T_{W,R} + T_{DAO,R}}{2} \right) + 273 \right)} \quad (3)$$

Eq. 4 estimates the temperature correction for losses at the winding at the current time step:

$$K_{W,1} = \frac{T_{W,1} + T_K}{T_{W,R} + T_K} \quad (4)$$

where $T_{W,R}$ is the rated value for average winding temperature rise and T_K is a temperature factor for resistance correction given in [23].

Eq. 4 is used to calculate the heat generated by the winding, $Q_{GEN,W}$, at the current time step:

$$Q_{GEN,W,1} = L_i^2 \left[P_W K_{W,1} + \frac{P_E}{K_{W,1}} \right] dt \quad (5)$$

where L is the load at this time step from the PHEV demand profile, P_W is the winding I^2R loss, P_E is the winding eddy loss, and dt is the size of the time step (1 minute for the purpose of this study). P_E and P_W are found or derived from the transformer specification sheet.

Eq. 1, 2, and 4 are used to calculate the heat lost by the windings, $Q_{lost,W}$, at the current time step:

$$Q_{LOST,W,1} = \left(\frac{T_{W,1} - T_{DAO,1}}{T_{W,R} - T_{DAO,R}} \right)^{\frac{5}{4}} \left(\frac{\mu_{W,1}}{\mu_{W,R}} \right)^{\frac{1}{4}} (P_W + P_E) dt \quad (6)$$

The winding mass times specific heat of windings, $M_W C_{pW}$, is estimated using Eq 7:

$$M_W C_{pW} = \frac{(P_W + P_E) \tau_W}{T_{W,R} - T_{DAO,R}} \quad (7)$$

where $T_{DAO,R}$ is the rated average oil at the top of the cooling ducts temperature and τ_W is the winding time constant in minutes. Annex G of [23] recommends five minutes as a value for τ_W .

Finally, the T_W at the next time step is estimated by Eq. 8, using Eq. 5, 6, and 7:

$$T_{W,2} = \frac{Q_{GEN,W,1} - Q_{LOST,W,1}}{M_W C_{pW}} + T_{W,1} \quad (8)$$

The average winding temperature from (8) is stored for use in the next iteration. Eq. (8) is a simplification of Eq. [XX] in [23].

2) *Average Oil Temperature Calculations:* The following parameters must be calculated to estimate the average oil temperature at the next time step. Additionally, an initial condition must be assumed for the average oil temperature, $T_{O,1}$, for the first time step.

Eq. 9 estimates the heat generated by stray losses, Q_S , at the current time step:

$$Q_{S,1} = \frac{L_1^2 P_S}{K_{W,1}} dt \quad (9)$$

where P_S are stray losses. The heat generated by core losses, Q_C , at the current time step are estimated with Eq. 10:

$$Q_{C,1} = P_C dt \quad (10)$$

where P_C are the core losses.

Eq. 11 estimates the heat lost by the oil to the ambient, $Q_{LOST,O}$, at the current time step:

$$Q_{LOST,O,1} = \left(\frac{T_{O,1} - T_{A,1}}{T_{O,R} - T_{A,R}} \right)^{\frac{1}{y}} (P_W + P_E + P_S + P_C) dt \quad (11)$$

where T_A is the current ambient temperature at this time step, $T_{A,R}$ is the rated ambient temperature, and $T_{O,R}$ is the rated average oil temperature.

Eq. 12 estimates the total mass times the specific heat of the tank, core, and oil:

$$\sum_{i=1}^n MCp = M_{TANK} C_{pTANK} + M_{CORE} C_{pCORE} + M_{oil} C_{p_{oil}} \quad (12)$$

where M_{TANK} , M_{CORE} , and M_{OIL} are the respective masses of the tank, core and oil and C_{pTANK} , C_{pCORE} , and $C_{p_{oil}}$ are the respective specific heats of the tank, core, and oil. The summation is performed from the first time instant, $i = 1$, to the final time instant, $n = 0$.

Finally, (9), (10), (11), and (12) are used to estimate the average oil temperature at the next time step:

$$T_{O,2} = \frac{Q_{LOST,W,1} + Q_S + Q_C - Q_{LOST,O,1}}{\sum MCp} + T_{O,1} \quad (13)$$

The average oil temperature from (13) is stored for use in the next iteration. Eq. (13) is a simplification of the equation in [23].

3) *Bottom Oil Temperature Calculations:* The following two calculations are required to estimate the temperature of the bottom oil, T_{BO} , at the current time step.

Eq. 14 estimates the oil temperature rise at the top of the transformer tank over the temperature at the bottom of the tank, ΔT_{TB} , at the current time step:

$$\Delta T_{TB,1} = \left(\frac{Q_{LOST,O,1}}{(P_W + P_E + P_S + P_C) dt} \right)^{z(T_{TO,R} - T_{BO,R})} \quad (14)$$

where Z is an exponent for top to bottom fluid temperature difference given in [23], and $T_{TO,R}$ & $T_{BO,R}$ are the rated top oil temperature and rated bottom oil temperature respectively. Eq. 14 from this time step and (13) from the previous time step are used to calculate, T_{BO} , at the current time step:

$$T_{BO,1} = T_{O,1} - \Delta T_{TB,1} \quad (15)$$

4) *Oil Adjacent to Hottest Spot Temperature Calculations:* The following calculations are required to estimate the oil adjacent to winding hottest spot temperature at the current time step. Eq. 16 estimates the oil temperature at the top of the cooling duct, T_{TDO} , at the current time step using (6) and (15):

$$T_{TDO,1} = \left(\frac{Q_{LOST,W,1}}{(P_W + P_E) dt} \right)^{x(T_{TDO,R} - T_{BO,R})} + T_{BO,1} \quad (16)$$

where $T_{TDO,R}$ is the rated oil temperature at the top of the cooling duct.

Eq. 19 estimates the temperature rise of oil at the winding hottest spot above the bottom oil, ΔT_{WO} , at the current time step:

$$\Delta T_{WO,1} = H_{HS} (T_{TDO} - T_{BO}) \quad (17)$$

where H_{HS} is the per unit winding height to hottest spot location, which Annex G of [23] recommends a value of one unless the actual value is known.

Finally, the oil adjacent to the winding hottest spot temperature, T_{WO} , at the current time instant is estimated using (15) and (17)

$$T_{WO,1} = T_{BO,1} + \Delta T_{WO,1} \quad (18)$$

5) *Winding Hottest Spot Temperature Calculations:* The winding hottest spot temperature, T_{HS} , is the final parameter to be estimated by the transformer temperature model. The following parameters are required for estimating T_{HS} . Additionally, an assumed initial condition for T_{HS} must be used for the first time step.

Eq. 19 uses (18) to estimate the oil viscosity for hottest spot calculation, μ_{HS} , at the current time step:

$$\mu_{HS,1} = Be^{C/\left(\frac{(T_{HS,1} + T_{WO,1})}{2} + 273\right)} \quad (19)$$

Eq. 20 estimates the rated oil viscosity for hottest spot calculation, $\mu_{HS,R}$:

$$\mu_{HS,R} = Be^{C/\left(\frac{(T_{HS,R} + T_{WO,R})}{2} + 273\right)} \quad (20)$$

where $T_{HS,R}$ and $T_{WO,R}$ are the rated winding hottest spot temperature and oil adjacent to winding hottest spot temperature, respectively.

Eq. 21 estimates the winding I^2R losses, P_{WHS} , at rated the winding hottest spot temperature at the current time step:

$$P_{WHS,1} = \left(\frac{T_{HS,R} + T_K}{T_{W,R} + T_K} \right) P_W \quad (21)$$

Eq. 22 estimates the eddy loss at the rated winding hottest spot temperature, P_{EHS} , at the current time step using (21):

$$P_{EHS,1} = E_{WHS} P_{WHS,1} \quad (22)$$

where E_{WHS} is the per unit I^2R loss at the winding hottest spot.

Eq. 23 calculates the temperature correction for losses at hot spot calculation, K_{HS} , at the current time step

$$K_{HS,1} = \left(\frac{T_{HS,1} + T_K}{T_{HS,R} + T_K} \right) \quad (23)$$

Eq. 24 estimates the heat generated by the windings at the hottest spot, $Q_{GEN,HS}$, at the current time step, using (21), (22), and (23):

$$Q_{GEN,HS,1} = L_i^2 \left[P_{WHS,1} K_{HS,1} + \frac{P_{EHS}}{K_{HS,1}} \right] dt \quad (24)$$

Eq. 25 estimates the heat lost by the windings at the hottest spot, $Q_{LOST,HS}$, at the current time step, using (8), (19), (20), (21), and (22):

$$Q_{LOST,HS,1} = \left(\frac{T_{HS,1} - T_{W,1}}{T_{HS,R} - T_{W,R}} \right)^{\frac{5}{4}} \left(\frac{\mu_{HS,1}}{\mu_{HS,R}} \right)^{\frac{1}{4}} (P_{WHS} + P_{EHS}) \quad (25)$$

Finally, from (12), (24), and (25), the winding hottest spot temperature is:

$$T_{HS,2} = \frac{Q_{GEN,HS,1} - Q_{LOST,HS,1}}{M_W C_{PW}} + T_{HS,1} \quad (26)$$

The average oil temperature from (26) is stored for use in the next iteration and will also be used in the next step of the PHEV transformer impact model, translating T_{HS} to transformer aging. Eq. (26) is a simplification of the equation in [23].

D. Translate Transformer Hot Spot Temperature to Transformer Aging

The transformer aging methodologies in this section are also based on IEEE C57.91-1995, as discussed in [24]. The winding hottest spot temperature is used to determine the transformer equivalent aging. The following equation for an aging acceleration factor, F_{AA} , is based on the equation for aging acceleration factor from [23]:

$$F_{AA,1} = e^{\left[\left(\frac{15000}{(T_{HS,1} + 273)} \right) - \left(\frac{15000}{(T_{HS,R} + 273)} \right) \right]} \quad (27)$$

The aging acceleration factor will have a value of 1.0 for continuous transformer operation at rated winding hottest spot temperature. For transformer operation above rated winding hottest spot temperature, the aging acceleration factor is greater than one, indicating accelerated aging. Eq. 28 estimates the total equivalent aging time, EQA , over the entire PHEV demand profile:

$$EQA = \sum_{i=1}^n F_{AA} dt \quad (28)$$

where the summation is performed from the first time instant, $i = 1$, to the final time instant, $n = 0$.

Eq. 29 estimates the equivalent aging factor, F_{EQA} , for the entire PHEV demand profile:

$$F_{EQA} = \frac{\sum_{i=1}^n F_{AA} dt}{\sum_{i=1}^n dt} \quad (29)$$

where the summations are performed from the first time instant, $i = 1$, to the final time instant, $n = 0$.

As with the discussion of (27), for continuous operation at rated winding hottest spot, the equivalent aging factor will have a value of 1.0. An equivalent aging factor greater than 1.0 indicates accelerated aging.

III. RESULTS

This study investigates transformer aging under various loading conditions, determined by the numbers of PEVs deployed and the number of houses serviced by the transformer. The study also accounts for transformer aging as a result of climate by running the PEV transformer impact model with annual temperature data from Los Angeles, CA and Burlington VT. This study assumes an equivalent base load profile for both Vermont and Los Angeles evaluations. As temperature is the free variable, it is important to note the difference between Burlington and Los Angeles climate. In general, Burlington temperatures fluctuate widely as compared to Los Angeles temperatures, which fluctuate within a much narrower temperature band. Although the maximum temperatures of both locations are quite similar, LA experiences significantly more warm days than Burlington.

In this study, two overhead distribution transformers are evaluated, a 15kVA and a 25kVA transformer. Each of the overhead distribution transformers are subject to both light and heavy annual loading. The 15kVA overhead distribution transformer services six homes during light annual loading and nine homes during heavy annual loading. The 25kVA overhead transformer services nine homes during light annual loading and twelve homes during heavy annual loading.

The load data used in the PEV transformer impact model is represented by a daily PEV demand profile displayed in Figure 2. The load data assumes a consistent daily load demand profile for each day of the year. Future work will incorporate varying daily demand profiles depending on time of year and separate weekend/weekday load profiles.

To illustrate the transformer aging represented by the PEV transformer impact model, Figure 3 provides a one day sample operation. This sample investigates a lightly loaded (6 home) 15kVA overhead distribution transformer on the hottest day of the Los Angeles temperature data (36 degree C max. temperature). Figure 3 displays the results for zero PEV deployment and five PEV deployment.

The results of running the PEV transformer impact model for one calendar year under each of the previously described scenarios are displayed in Figures 4-7. Specifically, the figures

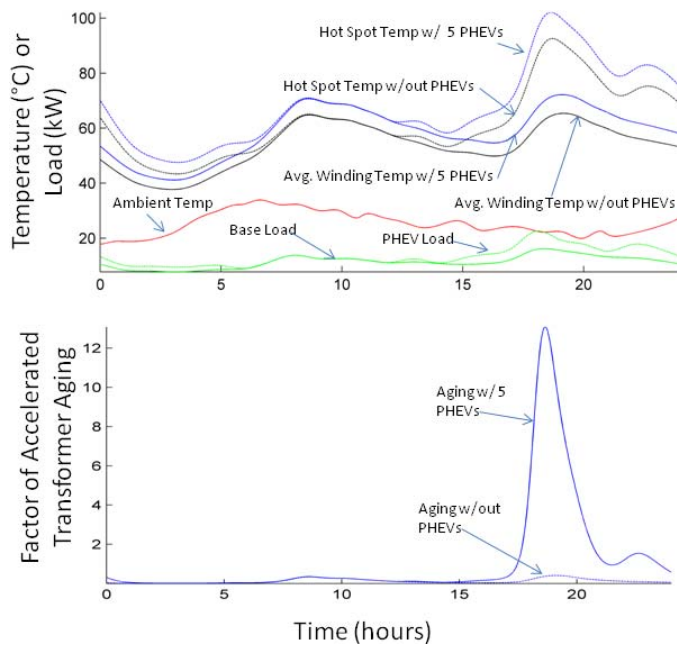


Figure 3. Illustration of PEV transformer impact model over the course of one day. The transformer modeled is a 15kVA overhead distribution transformer with a 6 home base load. The temperature data represents the hottest day in Los Angeles for 2009 (max. temp. 36 deg. C). The transformer is modeled under zero and 5 PEV deployment levels. Examined parameters are hot spot temperature, average winding temperature, ambient temperature, load, and factor of accelerated transformer aging.

illustrate the loss of life of the transformer (equivalent aging) and maximum winding hottest spot temperatures at each PEV deployment level. It is interesting to note that the transformer loss of life varies significantly between Los Angeles and Burlington climates though the maximum winding hottest spot temperature for each climate is approximately equivalent. The difference in transformer aging reflects the greater number of warm days in Los Angeles, discussed previously.

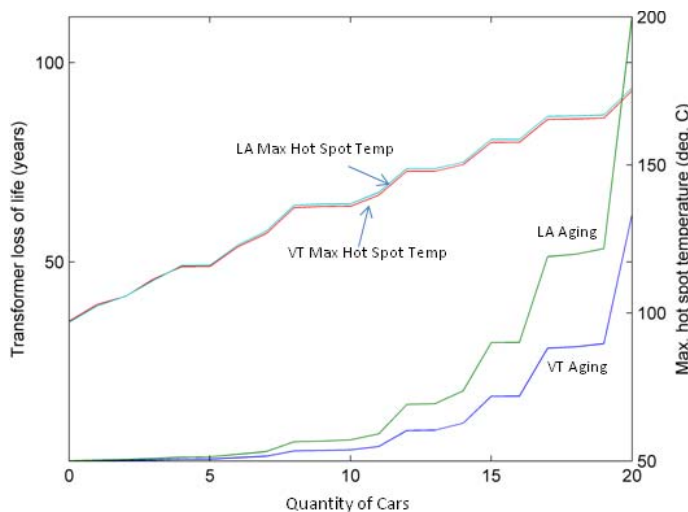


Figure 4. Loss of life (equivalent aging) and max. hot spot temperature results for 25kVA transformer, heavy annual loading (12 homes). PEV deployment levels range from zero to twenty.

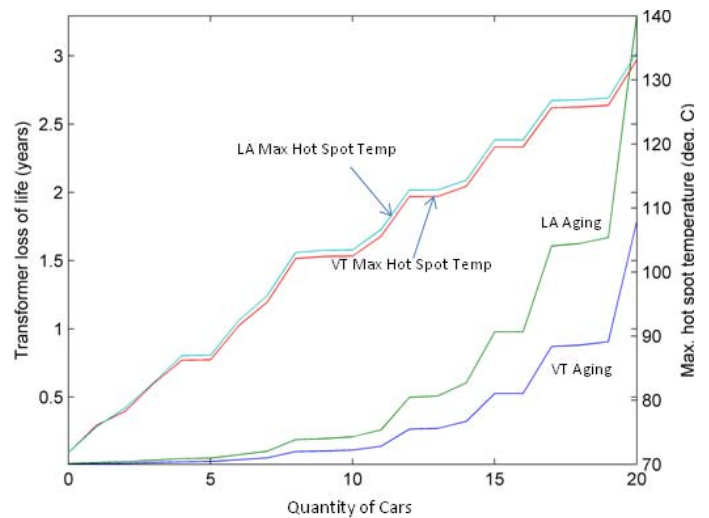


Figure 5. Loss of life (equivalent aging) and max. hot spot temperature results for 25kVA transformer, light annual loading (9 homes). PEV deployment levels range from zero to twenty.

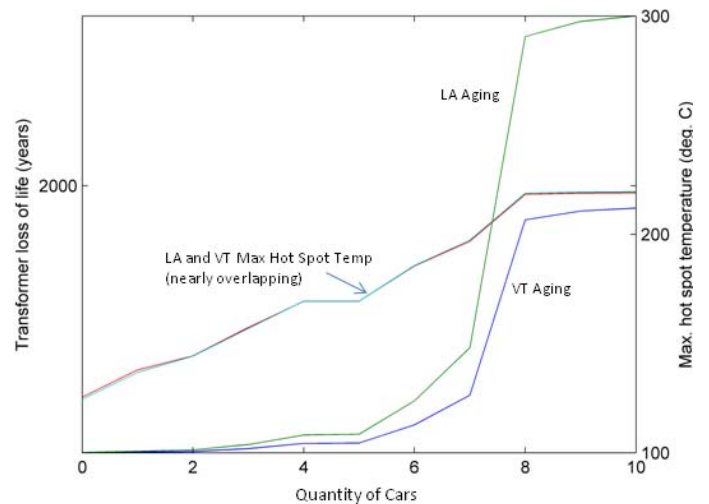


Figure 6. Loss of life (equivalent aging) and max. hot spot temperature results for 15kVA transformer, heavy annual loading (9 homes). PEV deployment levels range from zero to ten.

IV. CONCLUSIONS

This paper describes a method for combining the thermodynamic transformer model in IEEE C57.91 Annex G with empirical travel behavior data to estimate the impact of electric vehicle charging on residential distribution transformers. To illustrate the utility of our method we compare results for a lightly loaded and a heavily loaded residential transformer using temperature data for Vermont and Los Angeles. We find that for heavily loaded 15kVA transformers the addition of even as few as 5 PEVs, less than one car per household, is projected to increase the aging factor substantially, reducing the transformers expected lifetime to a year or less. We find that the heavily loaded 25kVA transformer can tolerate approximately 10 vehicles before the expected lifetime increases dramatically. We also notice a substantial difference in the aging results between Vermont and Los Angeles. While the maximum hot spot temperature is roughly the same between

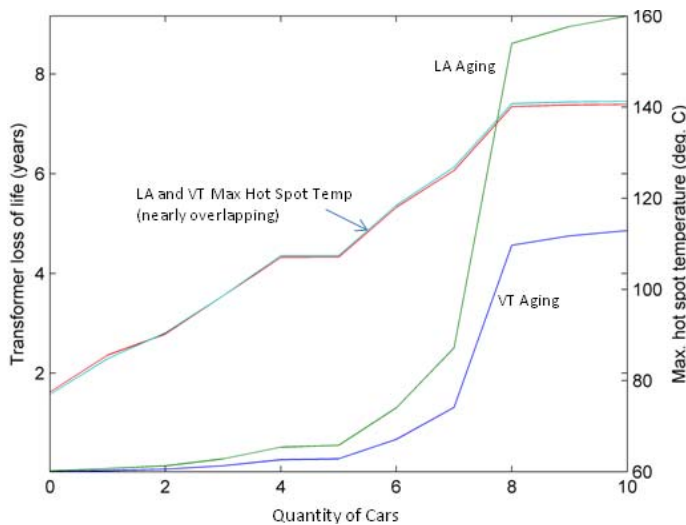


Figure 7. Loss of life (equivalent aging) and max. hot spot temperature results for 15kVA transformer, light annual loading (6 homes). PEV deployment levels range from zero to ten.

these two locations (both locations had similar maximum ambient temperatures) the number of hot days is far greater in the warmer climate, which substantially accelerates aging. This result highlights the need to consider temperature when developing transformer aging models.

In future work we plan to work on the development of decision tools to assist electric distribution utilities in determining the optimal replacement schedule for distribution infrastructure in regions with substantial PEV deployment.

REFERENCES

- [1] J. Kliesch and T. Langer, "Plug-in hybrids: An environmental and economic performance outlook," tech. rep., American Council for an Energy-Efficient Economy, Washington, DC, 2006.
- [2] EPRI, "Environmental assessment of plug-in hybrid electric vehicles: Volume 1: Nationwide greenhouse gas emissions," tech. rep., Electric Power Research Institute, 2007.
- [3] J. Gonder, T. Markel, M. Thornton, and A. Simpson, "Using global positioning system travel data to assess real-world energy use of plug-in hybrid electric vehicles," *Transportation Research Record*, 2007.
- [4] K. Parks, P. Denholm, and T. Markel, "Costs and emissions associated with plug-in hybrid electric vehicle charging in the xcel energy colorado service territory," tech. rep., National Renewable Energy Laboratory, Golden, CO, 2007.
- [5] C. Samaras and K. Meisterling, "Life cycle assessment of greenhouse gas emissions from plug-in hybrid vehicles: Implications for policy," *Environmental Science and Technology*, vol. 42, no. 9, pp. 3170–3176, 2008.
- [6] R. Sioshansi and P. Denholm, "Emissions impacts and benefits of plug-in hybrid electric vehicles and vehicle-to-grid services," *Environmental Science & Technology*, vol. 43, no. 4, pp. 1199–1204, 2009.
- [7] W. Kempton and J. Tomic, "Vehicle-to-grid power fundamentals: Calculating capacity and net revenue," *Journal of Power Sources*, vol. 144, no. 1, pp. 268–279, 2005.
- [8] M. J. Scott and M. Kintner-Meyer, "Impact assessments of plug-in hybrid vehicles on electric utilities and regional u.s. power grids part ii: Economic assesment," tech. rep., Pacific Northwest National Laboratory, 2007.
- [9] S. Hadley and A. Tsvetkova, "Potential impacts of plug-in hybrid electric vehicles on regional power generation," tech. rep., Oak Ridge National Laboratory, 2008.
- [10] P. Denholm and W. Short, "An evaluation of utility system impacts and benefits of optimally dispatched plug-in hybrid electric vehicles," Tech. Rep. NREL/TP-620-40293, National Renewable Energy Laboratory, 2006.

- [11] M. Kintner-Meyer, K. Schneider, and R. Pratt, "Impact assessments of plug-in hybrid vehicles on electric utilities and regional u.s. power grids part 1: Technical analysis," tech. rep., Pacific Northwest National Laboratory, 2007.
- [12] D. Crane and B. Prusnek, "The role of a low carbon fuel standard in reducing greenhouse gas emission and protecting our economy, state of california,," tech. rep., State of California, 2007.
- [13] A. E. Farrell and D. Sperling, "A low-carbon fuel standard for california part 2: Policy analysis, institute of transportation studies," tech. rep., University of California, Davis., 2007.
- [14] M. Zimmerman, "Plug-in electric vehicles get boost from bailout plan," 2008.
- [15] U. D. EIA, "Annual energy outlook 2010," tech. rep., U.S. Department of Energy, 2010.
- [16] M. E. Kahn and R. K. Vaughn, "Green market geography: The spatial clustering of hybrid vehicles and leed registered buildings," *The B. E. Journal of Economic Analysis & Policy*, vol. 9, no. 2, 2009.
- [17] C. Roe, F. Evangelos, J. Meisel, A. Meliopoulos, and T. Overbye, "Power system impacts of phev," in *Proceedings of the 42nd Hawaii International Conference on System Sciences*, (Waikoloa, HI), 2009.
- [18] C. Gerkenmeyer, M. Kintner-Meyer, and J. DeSteele, "Technical challenges of plug-in hybrid electric vehicles and impacts to the us power system: Distribution system analysis," tech. rep., Prepared for U.S. Dept. of Energy, Pacific Northwest National Laboratory, 2010.
- [19] J. F. Lindsay, "Temperature rise of an oil-filled transformer with varying load," *IEEE Transactions on Power Apparatus and Systems*, vol. PAS-109, no. 9, pp. 2530–2536, 1984.
- [20] S. Shao, M. Pipattanasomporn, and S. Rahman, "Challenges of phev penetration to the residential distribution network," in *Proceedings of the IEEE Power & Energy Society General Meeting*, (Minneapolis), July 2009.
- [21] L. P. Fernández, T. G. S. Román, R. Cossent, C. M. Domingo, and P. Frías, "Assessment of the impact of plug-in electric vehicles on distribution networks," *IEEE Transactions on Power Systems*, vol. in press, no. TPWRS-00985-2009, 2010.
- [22] K. Clement-Nyns, E. Haesen, and J. Driesen, "The impact of charging plug-in hybrid electric vehicles on a residential distribution grid," *IEEE Transactions on Power Systems*, vol. 25, pp. 371–380, Feb. 2010.
- [23] Transformers Committee of the IEEE Power Engineering Society, *IEEE Std C57.91-1995: IEEE Guide for Loading Mineral-Oil-Immersed Transformers*. IEEE, 1995.
- [24] L. Pierce, "Predicting liquid filled transformer loading capability," *IEEE Trans. on Industry Applications*, vol. 30, pp. 170–178, Jan/Feb 1994.
- [25] B. C. Lesieutre, W. H. Hagman, and J. L. Kirtley, "An improved transformer top oil temperature model for use in an on-line monitoring and diagnostic system," *IEEE Transactions on Power Delivery*, vol. 12, pp. 249–256, Jan 1997.
- [26] G. Swift, T. Molinski, and W. Lehn., "A fundamental approach to transformer thermal modeling—part 1: Theory and equivalent circuit," *IEEE Transactions on Power Delivery*, vol. 16, pp. 171–175, Apr 2001.
- [27] D. Lemoine and D. Kammen, "Effects of plug-in hybrids electric vehicles in california energy markets," in *Proceedings of the TRB 86th Annual Meeting*, 2007.
- [28] D. Wu, D. C. Aliprantis, and K. Gkritza, "Electric energy and power consumption by light-duty plug-in electric vehicles," *IEEE Transactions on Power Systems*, vol. in press, pp. Paper number: TPWRS-00890-2009, 2010.
- [29] ORNL, *2009 NHTS User Notes*. Oak Ridge National Laboratories, online: <http://nhts.ornl.gov/2009/pub/usernotes.pdf> ed., 2009.
- [30] "RELOAD Database Documentation and Evaluation and Use in NEMS [Online]. Available: <http://www.onlocationinc.com/LoadShapesReload2001.pdf>," tech. rep.
- [31] General Motors, "Chevrolet volt leads general motors into its second century,"
- [32] "About the karma, <http://www.fiskermiami.com/about-the-karma.htm>."
- [33] BYD, "F3dm specifications. <http://www.byd.com/showroom.php?car=f3dm..>"
- [34] K. Morrow and D. Karner, "Plug-in hybrid electric vehicle charging infrastructure review," tech. rep., U. S. Dept. of Energy, Idaho National Laboratory., 2008.

AUTHOR BIOGRAPHIES

PLACE
PHOTO
HERE

Alexander D. Hilshey is a graduate student in the School of Engineering at the University of Vermont. His research interests are power systems engineering.

PLACE
PHOTO
HERE

Paul D. H. Hines (S'95, M'07) is an Assistant Professor in the School of Engineering at the University of Vermont. He is also a member of the Carnegie Mellon Electricity Industry Center Adjunct Research Faculty and a commissioner for the Burlington Electric Department. He received the Ph.D. in Engineering and Public Policy from Carnegie Mellon U. in 2007 and the M.S. degree in Electrical Engineering from the U. of Washington in 2001. Formerly he worked at the US National Energy Technology Laboratory, where he participated in Smart Grid

research, the US Federal Energy Regulatory Commission, where he studied interactions between nuclear power plants and power grids, Alstom ESCA, where he developed load forecasting software, and for Black and Veatch, where he worked on substation design projects. His main research interests are in the areas of complex systems and networks, the control of cascading failures in power systems and energy security policy.

PLACE
PHOTO
HERE

Jonathan Dowds is a Research Assistant with the Transportation Research Center at the University of Vermont. He received a M.S. in Natural Resources in 2010 from the University of Vermont. His research interests include transportation sector energy use and the economics of cap-and-trade systems.